

Deciphering the transcriptional network of the dendritic cell lineage

Jennifer C Miller^{1,2}, Brian D Brown^{1,3}, Tal Shay⁴, Emmanuel L Gautier^{1,5,6}, Vladimir Jojic^{7,10}, Ariella Cohain³, Gaurav Pandey³, Marylene Leboeuf^{1,2}, Kutlu G Elpek⁸, Julie Helft^{1,2}, Daigo Hashimoto^{1,2}, Andrew Chow^{1,2,9}, Jeremy Price^{1,2}, Melanie Greter^{1,2,7}, Milena Bogunovic^{1,2}, Angelique Bellemare-Pelletier⁸, Paul S Frenette⁹, Gwendalyn J Randolph^{1,5,6}, Shannon J Turley⁸, Miriam Merad^{1,2} & the Immunological Genome Consortium¹¹

Although much progress has been made in the understanding of the ontogeny and function of dendritic cells (DCs), the transcriptional regulation of the lineage commitment and functional specialization of DCs *in vivo* remains poorly understood. We made a comprehensive comparative analysis of CD8⁺, CD103⁺, CD11b⁺ and plasmacytoid DC subsets, as well as macrophage DC precursors and common DC precursors, across the entire immune system. Here we characterized candidate transcriptional activators involved in the commitment of myeloid progenitor cells to the DC lineage and predicted regulators of DC functional diversity in tissues. We identified a molecular signature that distinguished tissue DCs from macrophages. We also identified a transcriptional program expressed specifically during the steady-state migration of tissue DCs to the draining lymph nodes that may control tolerance to self tissue antigens.

The Immunological Genome (ImmGen) Project is a consortium of immunologists and computational biologists from many institutions who have united to create an exhaustive database of gene-expression and regulatory-gene networks across the entire mouse hematopoietic lineage with the same rigorously controlled data-generation pipeline. With this extensive database, we sought to define the transcriptional profile and regulatory networks that control the homeostasis and function of the lineage development of dendritic cells (DCs). Discovered only 50 years ago, DCs are the most recent addition to the hematopoietic cell lineage¹. DCs represent a small population of hematopoietic cells that share properties with tissue macrophages, including their localization in most tissues and their ability to sample extracellular antigens, sense environmental injuries and contribute to the induction of tissue immune responses¹. However, in contrast to macrophages, whose main role is to scavenge damaged cells or pathogenic microbes and promote tissue repair, the main function of DCs is to initiate antigen-specific adaptive immune responses to foreign antigens that breach the tissues², as well as to maintain tolerance to self antigens³. The unique role of DCs in adaptive immunity relies on their ability to process and present self and foreign antigens in the form of complexes of peptide and major histocompatibility complex (MHC) class I and MHC class II on the cell surface^{4,5}, together with their superior ability to migrate to the tissue-draining lymph nodes⁶ and localize together with T lymphocytes and B lymphocytes⁷.

This makes DCs uniquely poised to control the induction of an antigen-specific immune response. However, controversies still exist about the overall distinction between DCs and macrophages because of their partially overlapping phenotypes and functions and, consequently, the exact contribution of macrophages and DCs to tissue immune responses is still debated^{8,9}.

DCs consist of distinct subsets with different abilities to process antigens, respond to environmental stimuli and engage distinct effector lymphocytes¹⁰. Classical DCs (cDCs) form the predominant DC subset and are further subcategorized as lymphoid tissue-resident CD8⁺ cDCs and CD8[−] cDCs¹¹. Lymphoid tissue-resident cDC subsets are functionally specialized; CD8⁺ cDCs excel in the cross-presentation of cell-associated antigens to CD8⁺ T cells, whereas CD8[−] cDCs are the most potent at stimulating CD4⁺ T cells. The second main subset of DCs are the plasmacytoid DCs (pDCs). The pDCs are uniquely able to produce large amounts of the antiviral cytokine interferon- α and initiate T cell immunity to viral antigens¹². Nonlymphoid-tissue DCs also include two cDC subsets: the CD103⁺ cDCs and the CD11b⁺ cDCs¹³. Similar to lymphoid-tissue CD8⁺ cDCs, nonlymphoid-tissue CD103⁺ cDCs are efficient cross-presenters of cell-associated antigens and are the most potent at stimulating CD8⁺ T cells¹⁰ but may also facilitate the induction of regulatory T cells in the intestine¹⁴.

The successive steps that lead to commitment to the DC lineage in the bone marrow are starting to be characterized. A myeloid

¹Immunology Institute, Mount Sinai School of Medicine, New York, New York, USA. ²Department of Oncological Sciences, Mount Sinai School of Medicine, New York, New York, USA. ³Department of Genetics and Genomic Sciences, Institute for Genomics and Multiscale Biology, Mount Sinai School of Medicine, New York, New York, USA. ⁴Broad Institute, Cambridge, Massachusetts, USA. ⁵Department of Regenerative Biology, Mount Sinai School of Medicine, New York, New York, USA. ⁶Department of Pathology & Immunology, Washington University in St. Louis, St. Louis, Missouri, USA. ⁷Computer Science Department, Stanford University, Stanford, California, USA. ⁸Cancer Immunology and AIDS, Dana Farber Cancer Institute, Boston, Massachusetts, USA. ⁹Albert Einstein College of Medicine, Bronx, New York, USA. ¹⁰Present address: Department of Computer Science, UNC, Chapel Hill, North Carolina, USA. ¹¹Full list of members and affiliations appears at the end of the paper. Correspondence should be addressed to M.M. (miriam.merad@mssm.edu).

Received 12 March; accepted 8 June; published online 15 July 2012; doi:10.1038/ni.2370

precursor cell called the ‘macrophage and DC precursor’ (MDP)¹⁵ has been identified and has been shown to give rise to monocytes and to the common DC precursor (CDP)¹⁶. CDPs are clonogenic precursor cells that have lost the potential to differentiate into monocytes or macrophages and give rise exclusively to pDCs and cDCs^{17,18}. CDPs also produce pre-cDCs, which are circulating cDC-restricted progenitor cells that have lost the potential to differentiate into pDCs¹⁶ and home to tissues to differentiate locally into lymphoid tissue–resident CD8⁺ or CD8[−] cDCs¹⁶ and nonlymphoid tissue–resident cDCs¹⁹. Although much progress has been made in understanding the ontogeny and function of DCs, the transcriptional regulation of commitment to the DC lineage and the diversification and functional specialization of DCs *in vivo*, as well as the relationship between lymphoid-tissue DCs and nonlymphoid-tissue DCs, remain poorly understood. These questions remain unanswered in part because of the limited data available for comprehensive, comparative analysis both vertically and horizontally across the immune system.

Here we delineate the transcriptional network of DC progenitor cells, lymphoid-tissue and nonlymphoid-tissue DCs, as well as nonlymphoid-tissue DCs in a migratory state. The results of our study help characterize a DC-specific signature that distinguishes cDCs from macrophages in tissues. Our study identifies the lineage relationship between various tissue DC subsets as well as the predicted regulators of tissue DC diversity. Our results also identify a signature of genes expressed by all nonlymphoid-tissue cDCs that have migrated to the draining lymph nodes, regardless of their tissue or lineage origin.

RESULTS

Transcriptional characterization of the DC lineage

We characterized 26 distinct DC populations isolated from primary lymphoid tissues, secondary lymphoid tissues and nonlymphoid tissues on the basis of expression of markers on the cell surface thought to represent discrete DC subsets with specialized immunological function *in vivo*¹³ (Table 1). We sorted each subset to high purity according to the standard operating protocol of the ImmGen Project. We isolated CD8⁺ and CD8[−] cDCs and pDCs from the spleen, thymus and lymph nodes; purified CD103⁺ cDCs and CD11b⁺ cDCs from the lung, liver, small intestine and kidney; and isolated epidermal Langerhans cells (LCs) from the epidermis. We isolated tissue-migratory CD103⁺ DCs and CD11b⁺ DCs from tissue-draining lymph nodes. We purified granulocyte-macrophage precursors (GMPs), MDPs and CDPs from the bone marrow and isolated circulating monocytes from the blood. We double-sorted cell populations to a purity of over 99% on the basis of the appropriate cell surface markers (Table 1). We did the final sorting by flow cytometry (10,000–30,000 cells) directly in TRIzol, froze the samples after 2 min and sent them to the core team of the ImmGen Project in Boston, Massachusetts. RNA was prepared from the TRIzol lysate and hybridized to microarrays as described²¹. Expression profiling data were generated on Affymetrix ST1.0 microarrays according to the ImmGen Project pipeline, with data generation and quality control as described before²¹. The purified DC subsets were isolated from laboratories in New York, New York, and Boston, Massachusetts. One population of spleen DCs (population 1, sorted in New York) was sorted on the basis of expression of MHC class II and CD11c and lack of expression of F4/80 or B220 and was found to be identical to spleen DCs (population 2, sorted in Boston) purified mainly on the basis of CD11c expression. For analysis of whether site or batch effects may have confounded the signals, CD8⁺ and CD8[−] spleen cDCs were sorted independently at

the two different locations (New York and Boston). The data showed excellent correlation in each subset, with little evidence of lab-specific influences, for the differences between CD8[−] and CD8⁺ cDC subsets (Supplementary Fig. 1).

Transcriptional control of commitment to the DC lineage

The commitment of cells of the myeloid lineage to the mononuclear phagocyte lineage is determined at the stage of the MDP, at which point erythroid, megakaryocyte, lymphoid and granulocyte fates have been precluded^{15,16,22}. DC commitment occurs during the transition from MDP to CDP, with the loss of monocyte potential¹⁶, whereas cDC commitment occurs at the pre-cDC stage, with the loss of pDC potential^{17,18}. We probed the pattern of regulator expression along the myeloid-DC lineage tree to search for transcriptional activators and repressors that correlated with each differentiation step and thereby identified groups of genes encoding regulators that were induced at different stages during DC differentiation. The first group was upregulated specifically during the differentiation of GMPs into MDPs (expression 1.5-fold or more higher in MDPs than in GMPs; Fig. 1a, i), which would potentially influence the global development of DCs and macrophages. This group included *Sox4* and *Taf4b*, which encode transcription factors known to have a role in cell fate and the initiation of transcription, respectively. The second group was upregulated during the transition from MDP or GMP to CDP (expression 1.5-fold or more higher in CDPs than in MDPs or GMPs) but not during the differentiation of MDPs into circulating monocytes (Fig. 1a, ii) and encoded molecules that probably control CDP-versus-monocyte fate. This group included genes encoding molecules known to regulate pDC development, such as *Irf8*, *Bcl11a* and *Runx2*, as well as low expression of *Zbtb46* (which encodes zinc-finger transcription factor Zbtb46). A third group was downregulated (67% lower expression; Fig. 1a, iii) during the transition from GMP to MDP and included *Tgfb1* (a homeobox gene induced by transforming growth factor-β (TGF-β)), *Tcfec* (which encodes a transcription factor) and *Trim13* (which encodes an E3 ubiquitin ligase). To search for regulators that might contribute to the pDC-versus-cDC fate of CDPs, we examined the expression of candidate genes encoding regulators during the differentiation of CDPs into pDCs, lymphoid-tissue CD8⁺ cDCs or lymphoid-tissue CD8[−] cDCs (Supplementary Fig. 2). The differentiation of CDPs into pDCs was associated with the downregulation of *Id2*, *Zbtb46* and *Cited2* (which encodes a regulator of TGF-β), whereas the differentiation of CDPs into cDCs was associated with the downregulation of *Irf8*, *Tcf4* and *Runx2* and upregulation of *Batf3*, *Bcl6* and *Ciita* (which all encode transcription factors). We also identified genes encoding transcription factors that were upregulated 1.5-fold or more in CD8⁺ cDCs relative to their expression in CD8[−] cDCs (and vice versa). These included expected genes such as *Irf8*, which encodes the CD8⁺ cell- and CD103⁺ cell-specific transcription factor IRF8 (refs. 19–23), as well as *Pbx1*, which encodes a Hox transcription factor shown to function during definitive hematopoiesis in fetal liver²⁴.

Several transcription factors identified in our analysis have been shown to control DC development. For example, the differentiation of pDCs and cDCs is dependent on the zinc-finger protein Ikaros²⁵, the cytokine receptor Flt3 and its ligand Flt3L²⁶ (and Flt3 expression is partly controlled by the transcription factor PU.1 (encoded by *Sfp1*)²⁷), and the transcription factor STAT3, which is activated by Flt3 signaling and mediates Flt3L-dependent DC differentiation²⁸. Factors that regulate DC diversification are also starting to be identified. The transcription factors E2-2 (encoded by *Tcf4*), Spi-B and

Table 1 Expression of cell surface markers by DCs and DC precursor populations

		Marker																		Replicate Number	
Population	Location	CD45	MHCII	CD11c	CD8	CD4	CD11b	CD103	F4/80	Gr-1	B220	Sca-1	c-Kit	CSF1R	Flt3	CD3	CD19	Ter119	NK1.1		Other
Lymphoid-tissue DCs																					
Resident DCs																					
CD8 ⁺	SDLN	+		+	+	-	-			-						-	-	-	-	-	3
	MLN	+		+	+	-	-			-						-	-	-	-	-	3
	Spleen (NY)	+	+	+	+	-	-		-		-						-	-	-	-	3
	Spleen (MA)	+		+	+	-	-									-	-	-	-	-	5
	Thymus	+	+	+	+	-	-	+			-					-	-	-	-	-	3
CD8 ⁻	SDLN	+		+	-	+	+			-						-	-	-	-	-	3
	MLN	+		+	-	+	+			-						-	-	-	-	-	2
	Spleen (NY)	+	+	+	-	+			-		-						-	-	-	-	6
	Spleen (MA)	+		+	-	+	+			-						-	-	-	-	-	5
	Spleen	+		+	-	-	+			-						-	-	-	-	-	3
Migratory DCs																					
CD103 ⁺	SDLN	+	hi	int	-	-	-	+												Lang ⁺	3
	MLN	+	hi	int	-	-	-	+													3
CD11b ⁺	SDLN	+	hi	int	-	-	+	-												Lang ⁻	3
	MLN	+	hi	int	-	-	+	-													3
LC	SDLN	+	hi	int	-	-	+	-												Lang ⁺	3
pDC																					
	Spleen	+		+	+					+	+					-	-		-		3
	MLN	+		+	+					+	+					-	-		-		2
	SDLN	+		+	+					+	+					-	-		-		3
	Spleen	+		+	-					+	+					-	-		-		3
Nonlymphoid-tissue DCs																					
CD103 ⁺	Lung	+	+	+			-	+													5
	Liver	+	+	+	-	-	-	+											-		2
	SI	+	+	+	-	-	-	+	-												4
CD11b ⁺	Lung	+	+	+			+	-													2
	Liver	+	+	+	-	-	+	-											-		3
	SI	+	+	+	-	-	+	-	+												7
	Kidney	+	+	+			+	-	lo	-										NKp46.1 ⁻	3
CD103 ⁺ CD11b ⁺	SI	+	+	+	-	-	+	+	-	-											4
LCs	Skin	+	+	+	-	-	+	-											-	Lang ⁺	2
Precursors																					
GMPs	BM						-			-	-	-	hi			-		-	-	CD34 ⁺ & CD16-CD32 ^{hi}	3
MDPs	BM						-			-	-	-	hi	+	+	-		-			3
CDPs	BM						-			-	-	-	lo	+	+	-		-			3
Monocyte	Blood		-							+	-			+						CD43 ⁻	3

Expression of cell-surface markers by DCs purified by flow cytometry from the bone marrow (precursor cells) or tissues (differentiated cells) according to standard operation procedures of the ImmGen Project. The spleen pDCs include a CD8⁺ subset and a CD8⁻ subset. CSF1R, colony-stimulating factor 1 receptor; Lang, langerin; BM, bone marrow; NY and MA, DCs isolated from laboratories in New York, New York, and Boston, Massachusetts, respectively. Data are representative of at least three experiments.

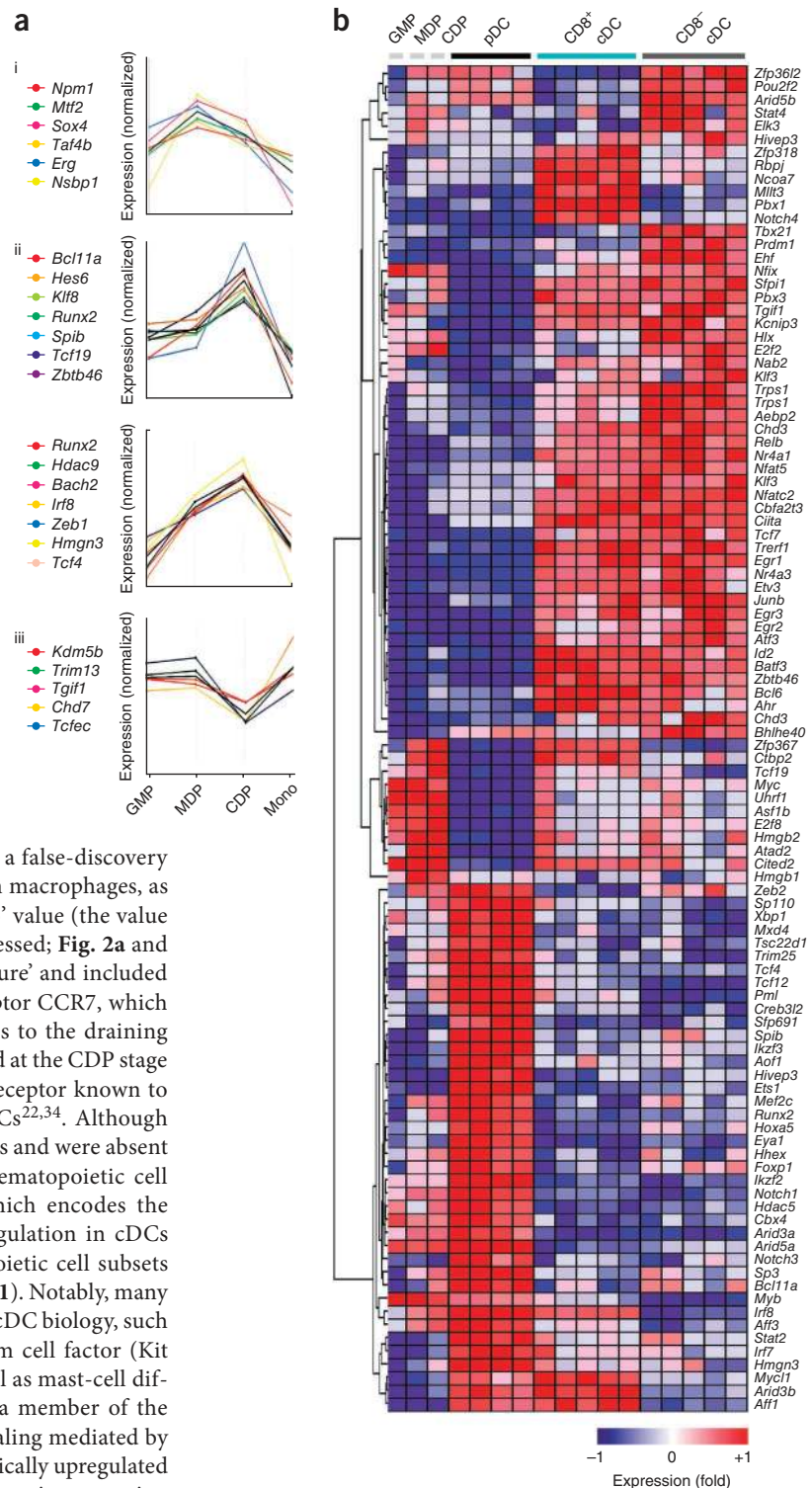
IRF8 have been shown to control pDC differentiation²⁹, whereas Bcl-6 controls the development of cDCs but not of pDCs³⁰ in the spleen. The transcription factors BATF3, IRF8, Id2 and mTOR control the development of CD8⁺ cDCs and CD103⁺ cDCs, whereas the differentiation of CD8⁻ cDCs is controlled by the transcription factors IRF2, IRF4 (ref. 8) and Notch2 (ref. 20), a factor that also controls the differentiation of intestinal CD103⁺CD11b⁺ cDCs²⁰. Consistent with our finding that *Zbtb46* expression was associated with the commitment of CDPs to the cDC lineage, two published studies have shown that *Zbtb46* expression is restricted to cDC-committed precursor cells and tissue cDCs and that *Zbtb46* can serve as a useful marker for distinguishing cDCs from other tissue phagocytes^{31,32}. Together these results provided a map of known regulators and also previously unknown potential regulators that accompanied key checkpoints in the generation of DCs and helped to identify the molecular cues that control differentiation into the monocyte or DC lineage as well as DC diversification *in vivo*.

Identification of a cDC core gene signature

One of the main challenges in understanding the exact contribution of cDCs versus macrophages in tissue immunity has been the lack of specific phenotypic markers for defining tissue cDCs. We first ascertained whether cDCs and macrophages sorted on the basis of published markers clustered as one population or as separate populations by principal-component analysis (PCA) of the 15% of genes with the most variable expression by various steady-state leukocytes isolated from the same organ (**Supplementary Fig. 1d**). These results showed that macrophages and cDCs formed distinct populations at the transcriptome level.

We then sought to determine whether cDCs expressed a set of genes present in all cDC subsets but absent from macrophages. As nonlymphoid-tissue CD11b⁺ cDCs probably form a heterogeneous population^{8,9}, we excluded those cells from our comparative analysis and investigated whether lymphoid-tissue CD8⁺ cDCs and CD8⁻ cDCs and nonlymphoid-tissue CD103⁺ cDCs shared specific cDC transcripts absent from four prototypical macrophage populations

Figure 1 Expression of genes encoding transcription factors along the DC lineage. (a) Kinetics of the expression of genes encoding transcriptional regulators upregulated 1.5-fold or more in MDPs relative to their expression in GMPs (i) or upregulated 1.5-fold or more in CDPs relative to their expression in MDPs and/or GMPs (ii) or, conversely, 1.5-fold or higher in MDPs relative to their expression in CDPs (iii), normalized to mean expression across all samples and grouped in plots by common patterns of gene expression across the GMP, MDP, CDP and monocyte (Mono) families. There were two transcripts for *Runx2* and both are presented here. (b) Heat map of the results in a, along with those of transcripts upregulated by at least 1.5-fold at each cellular checkpoint relative to their expression in the nearest developmental neighbor of that checkpoint (cDCs versus pDCs, and CD8⁺ cDCs versus CD8⁺ cDCs; **Supplementary Fig. 2**); results were log-transformed, normalized (to the mean expression of zero across samples) and centered, and populations and genes were clustered by pairwise centroid linkage with the Pearson correlation. Data are representative of at least three experiments with three or more replicates (unless noted otherwise in **Table 1**).



profiled by the ImmGen Project (Online Methods). We found 24 genes expressed in cDCs (with a change in expression of two-fold or more between cDC and macrophages, and a false-discovery rate (FDR) of 0.05 or less (*t*-test)) and absent from macrophages, as determined by expression values below the 'QC95' value (the value at which the gene has a 95% chance of being expressed; **Fig. 2a** and **Table 2**). This group formed the 'core cDC signature' and included the gene (*Ccr7*) that encodes the chemokine receptor CCR7, which has been shown to control the migration of cDCs to the draining lymph nodes³³; *Zbtb46*, which was first upregulated at the CDP stage (**Fig. 1a**); and *Flt3*, which encodes the cytokine receptor known to control the differentiation and homeostasis of DCs^{22,34}. Although many of the genes that showed enrichment in cDCs and were absent from macrophages were also present in other hematopoietic cell populations, *Zbtb46*, *Flt3*, *Pvrl1* and *Anpep* (which encodes the aminopeptidase CD13) showed substantial upregulation in cDCs relative to their expression in all other hematopoietic cell subsets (**Supplementary Fig. 3** and **Supplementary Table 1**). Notably, many genes encoded products with no identified role in cDC biology, such as *Kit*, which encodes c-Kit, the receptor for stem cell factor (Kit ligand), known for its role in hematopoiesis as well as mast-cell differentiation³⁵, and *Btla*, which encodes CD272, a member of the immunoglobulin superfamily that attenuates signaling mediated by B cell and T cell antigen receptors³⁶. *Btla* was specifically upregulated in CD8⁺ cDC and CD103⁺ cDC populations relative to its expression in CD8[−] cDCs (**Fig. 2, Supplementary Fig. 3** and **Supplementary Table 1**). Several genes were upregulated twofold or more (FDR ≤ 0.05 (*t*-test)) in cDCs relative to their expression in macrophages, including many genes encoding MHC class II molecules, as well as *Dpp4* (**Fig. 2a** and **Table 3**), which encodes the dipeptidyl peptidase CD26, whose role in DC function remains unclear. By flow cytometry, we confirmed that *Flt3*, c-Kit, the inhibitory receptor CD272 (BTLA) and CD26 were expressed as proteins on spleen CD8⁺ cDCs and spleen CD8[−] cDCs, as well as nonlymphoid-tissue CD103⁺ cDCs, and were

absent from red-pulp macrophages, lung alveolar macrophages, peritoneal macrophages and microglia (**Fig. 2b**). Together these results identified a core DC signature that helped distinguish tissue DCs from macrophages in tissues.

Unique gene signatures of distinct tissue DC clusters

DC subsets are classified on the basis of distinct cell-surface markers, and different subsets exist in lymphoid and nonlymphoid tissues. To understand the relationships among these various DCs populations,

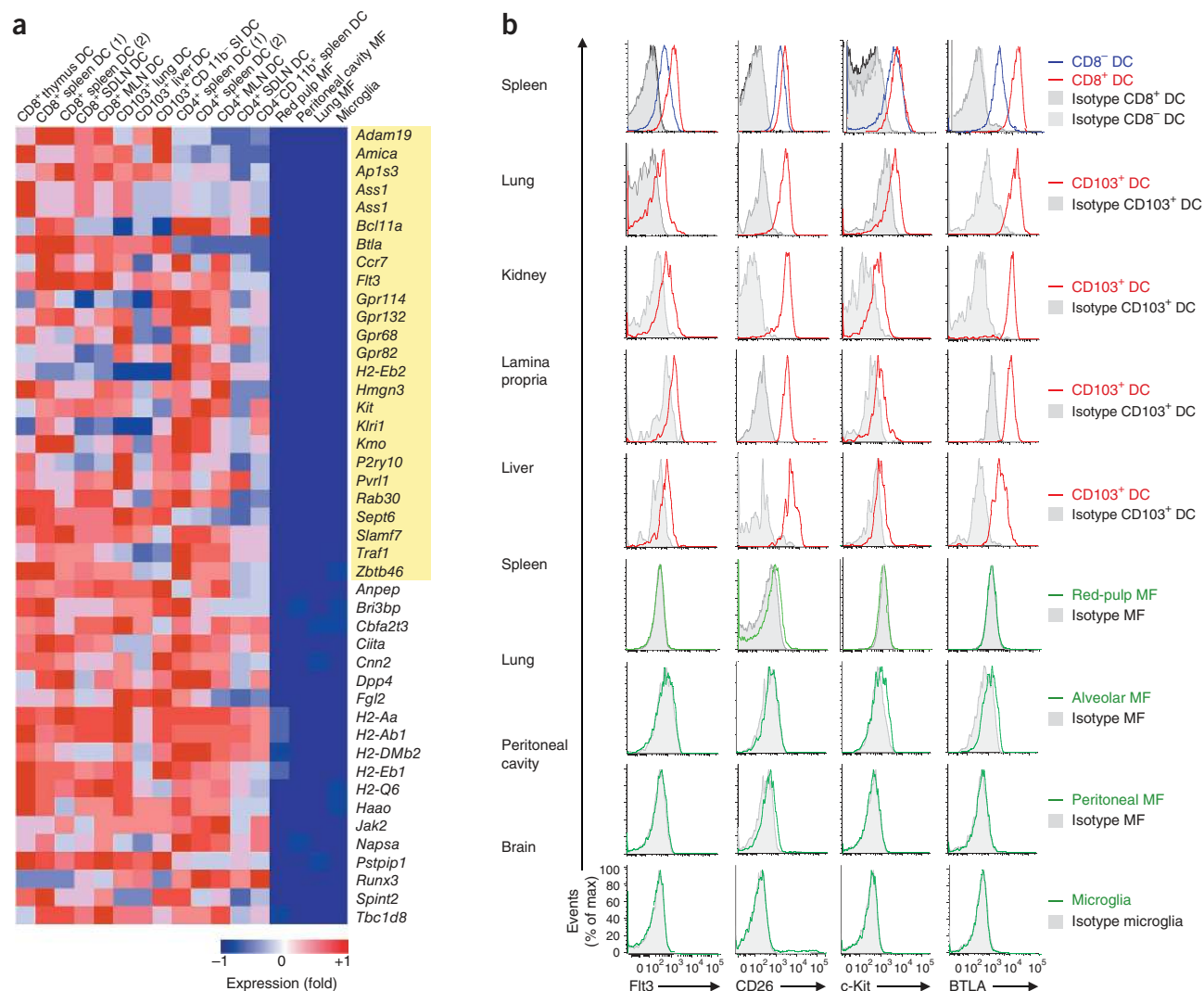


Figure 2 Identification of genes significantly upregulated in cDCs relative to their expression in macrophages. **(a)** Heat map of transcripts with different expression in lymphoid-tissue cDCs and nonlymphoid-tissue CD103⁺ cDCs than in four prototypical macrophage populations (values, **Tables 2 and 3**; presented as in **Fig. 1b**). Yellow highlighting indicates transcripts expressed in cDCs and absent from macrophages according to the QC95 value; these form the core cDC signature. SDLN, skin-draining lymph node; MLN, mesenteric lymph node; SI, small intestine; MF, macrophage; (1), sample from New York, New York; (2), sample from Boston, Massachusetts. **(b)** Flow cytometry of single-cell suspensions of the spleen, lung, kidney, lamina propria, liver, peritoneal cavity and brain, assessing the expression of Flt3, CD26, c-Kit and BTLA in gated spleen CD8⁺ cDCs or CD8[−] cDCs, tissue CD103⁺ cDCs and tissue macrophage populations. Isotype (grey shaded curves), isotype-matched control antibody. Data are representative of three independent experiments with three or more replicates (unless noted otherwise in **Table 1**).

we did PCA of the 15% of genes with the most variable expression in populations of lymphoid-tissue pDCs (from the spleen, skin-draining lymph nodes and mesenteric lymph nodes), lymphoid-tissue cDCs (lymph node, spleen and thymus CD8⁺ cDCs; lymph node and spleen CD8[−]CD4⁺ cDCs; and spleen CD8[−]CD4[−]CD11b⁺cDCs) and nonlymphoid-tissue CD103⁺ cDCs (from the lung, liver and small intestine). The main principal components identified three distinct DC clusters: one cluster was formed by lymphoid-tissue CD8⁺ cDCs and nonlymphoid-tissue CD103⁺ cDCs, a second cluster was formed by lymphoid-tissue CD8[−] cDCs and a third cluster was formed by pDCs (**Fig. 3a**). We used these clusters to define specific gene-expression signatures. The pDC cluster expressed 93 genes absent from other cDCs, whereas the two cDC clusters expressed 125 genes absent from pDCs, including *Zbtb46*, *Pvrl1* and *Anpep* (**Fig. 3b**, **Supplementary Fig. 4** and **Supplementary Table 1**). Further analysis of the two cDC subsets showed 28 genes shared by CD8⁺ cDCs and CD103⁺ cDCs

and absent from other cDCs (**Fig. 3b**, **Supplementary Figs. 3 and 4** and **Supplementary Table 1**). Genes specific to CD8⁺ cDCs and CD103⁺ cDCs included *Thr3* (which encodes Toll-like receptor 3 (TLR3)) and *Xcr1* (which encodes the chemokine receptor CXCR1). In agreement with their unique expression of TLR3, CD8⁺ cDCs and CD103⁺CD11b[−] cDCs share a superior ability to respond to TLR3 ligands^{37–40}. In addition, published data have shown that CD8⁺ DCs are also the only lymphoid-tissue DC subset that produces interferon- λ in response to the TLR3 ligand poly(I:C)⁴¹, and we have obtained similar results for lung CD103⁺CD11b[−] DCs (J.H. and M.M., data not shown). Notably, *Xcr1* (encoding CXCR1, which controls the differentiation of CD8⁺ T effector cells in mice and humans^{42,43}) was expressed only in CD8⁺ cDCs and CD103⁺ cDCs across the entire hematopoietic cell lineage (**Supplementary Fig. 4c** and **Supplementary Table 1**). Lymphoid-tissue CD8[−] cDCs populations coexpressed core cDC genes together with several genes specific to monocytes and macrophages

Table 2 Core cDC transcripts

Gene	cDC expression	Macrophage expression
<i>Adam19</i>	1,119 ± 259.2	94.3 ± 6.1
<i>Amica1</i>	702.6 ± 216.9	45.5 ± 3.1
<i>Ap1s3</i>	642.4 ± 111.2	43.7 ± 7.1
<i>Ass1</i>	905 ± 234.2	69.8 ± 2
<i>Bcl11a</i>	940.1 ± 262.9	95.3 ± 9.3
<i>Btla</i>	1,481.7 ± 413.3	49.4 ± 3.9
<i>Ccr7</i>	1,012 ± 251.5	81.3 ± 7.2
<i>Flt3</i>	3,408.4 ± 370.3	66.3 ± 11
<i>Gpr114</i>	406.6 ± 132.9	57.1 ± 3.9
<i>Gpr132</i>	1,007.6 ± 127.9	84.1 ± 5.2
<i>Gpr68</i>	289.4 ± 61.4	52.5 ± 4.8
<i>Gpr82</i>	67.7 ± 18.2	11.7 ± 0.8
<i>H2-Eb2</i>	782.2 ± 371.1	43.4 ± 5.5
<i>Hmgn3</i>	153.6 ± 25.3	23.1 ± 2.5
<i>Kit</i>	2,368.3 ± 375.7	67.7 ± 6.1
<i>Klri1</i>	527.4 ± 204.7	17.2 ± 0.5
<i>Kmo</i>	1,160.4 ± 212.6	20.7 ± 1.1
<i>P2ry10</i>	519.2 ± 152.7	19.6 ± 2.2
<i>Pvrl1</i>	475.6 ± 54.3	74.4 ± 6.1
<i>Rab30</i>	289.2 ± 52.8	28.7 ± 3.6
<i>Sept6</i>	1,080.3 ± 202.3	99.2 ± 12.4
<i>Slamf7</i>	1,727.4 ± 145.6	31.7 ± 5.2
<i>Traf1</i>	1,044.4 ± 224.5	51.6 ± 2.8
<i>Zbtb46</i>	400.8 ± 54.2	93.8 ± 10.3

Genes of the transcriptome expressed in cDCs (excluding nonlymphoid-tissue CD11b⁺ cDC subsets; FDR ≤ 0.05 (t-test)) and not expressed in macrophages (four macrophage populations: red-pulp, alveolar and peritoneal-cavity macrophages and microglia), according to the QC95 value; results are presented as 'relative expression units'. Data are representative of at least three experiments (average ± s.e.m.).

(Supplementary Fig. 4 and Supplementary Table 1), consistent with published results showing that CD8⁺ cDCs consist of two subsets with different expression of macrophage-related genes²⁰. However, some genes, including *Dscam* (which encodes the adhesion molecule Dscam), were expressed only by CD8⁺ cDCs and were not expressed in macrophages or monocytes (Supplementary Fig. 4 and Supplementary Table 1). *Dscam* has enormous molecular diversity and is involved in axon guidance⁴⁴ and pathogen recognition⁴⁵.

To delineate the gene 'architecture program' of these subsets of DCs, we searched among the 334 fine modules of genes with substantial coexpression and their predicted regulators identified for the entire ImmGen Project compendium (<http://www.immgen.org/ModsRegs/modules.html>) to identify those with significant upregulation in specific DC subsets relative to their expression in the rest of the samples from the ImmGen Project (Fig. 3c–e). Module 150 showed significant upregulation in pDCs ($P = 4.77 \times 10^{-11}$), and predicted regulators of this module included IRF8, STAT2, Runx2 and Egr5 (encoded by *Tsc22d1*; Fig. 3c), whose genes were also expressed during the commitment of CDP to pDCs (Fig. 1b and Supplementary Fig. 2). Module F156 showed significant upregulation in cDCs ($P = 7.01 \times 10^{-35}$) and significant enrichment for core cDC genes ($P = 4.18 \times 10^{-10}$ (hypergeometric test)), such as *Zbtb46* and *Pvrl1*. Predicted regulators of this module included BATF3 and RelB (Fig. 3d), whose genes were also upregulated during the commitment of CDPs to cDCs (Fig. 1b and Supplementary Fig. 2). Module 152 showed significant upregulation in CD8⁺ cDCs and CD103⁺ cDCs ($P = 1.34 \times 10^{-25}$) and enrichment for genes of the CD8⁺ DC and CD103⁺ DC transcript signature ($P < 1 \times 10^{-13}$ (hypergeometric test)), such as *Tlr3*, *Xcr1* and *Fzd1* (Fig. 3e). IRF8 and Pbx-1, encoded by genes upregulated in CD8⁺ cDCs relative to their expression in CD8⁺ cDCs (Fig. 1b), were predicted regulators of this module (Fig. 3e). Module 154 showed significant upregulation in CD8⁺ cDCs ($P = 1.08 \times 10^{-15}$) and in intestinal CD103⁺ CD11b⁺ cDCs, a nonlymphoid-tissue cDC subset that

has been shown to share development properties with lymphoid-tissue CD8⁺ cDCs²⁰ (Supplementary Fig. 5). These modules, together with the core gene signature, identified previously unknown genes as well as potential regulators of DC functional specialization *in vivo*.

CD11b⁺ DC heterogeneity delineates the cDC core gene signature

Nonlymphoid-tissue CD11b⁺ cDCs remain the least-well-characterized cDC subset both ontogenically and functionally. The small intestine is populated by three phenotypically distinct cDC subsets with different expression of the integrins CD103 and CD11b. CD103⁺CD11b⁺ cDCs and CD103⁺CD11b⁺ cDCs are derived from CDPs and pre-DCs^{46,47}, require Flt3L for their development⁴⁷, migrate efficiently to the draining lymph nodes⁴⁸ and are thought to represent cDCs⁴⁹. In contrast, the CD103⁺CD11b⁺ subset derives from circulating monocytes^{46,47}, develops independently of Flt3L, requires the ligand for colony-stimulating factor 1 receptor for its development⁴⁷, migrates poorly to the draining lymph nodes⁴⁸ and is thought to relate more closely to macrophages than to cDCs⁴⁹.

To determine whether those subsets had differences in their expression of genes of the core cDC signature identified above, we purified CD103⁺CD11b⁺, CD103⁺CD11b⁺ and CD103⁺CD11b⁺ cDC subsets from the small intestine, as well as CD11b⁺ cDCs from the lung, liver and kidney, and did PCA of those along with the rest of the cDC subsets and with macrophages isolated from the spleen, lung, brain and peritoneum. The CD11b⁺ cDC subsets were distributed across the PCA plot between the cDCs and macrophages (Fig. 4a) and expressed a variable number of cDC core genes (Fig. 4b), which indicated that nonlymphoid-tissue CD11b⁺ cDCs, as defined at present, represented a heterogeneous population.

In the PCA plot, CD103⁺CD11b⁺ cDCs from the small intestine clustered with the CD8⁺ cDCs and CD103⁺ cDCs, whereas CD103⁺CD11b⁺ cDCs from the lamina propria of the small intestine clustered near lymphoid CD8⁺ cDCs and did not express unique transcripts of CD8⁺ cDCs and CD103⁺ cDCs (Fig. 4a and Supplementary Fig. 6). Accordingly, CD103⁺CD11b⁺ cDCs from the small intestine expressed all transcripts specific to the CD8⁺ cDCs and CD103⁺ cDCs identified (Fig. 3), including *Fzd1*, which encodes a Wnt-receptor signaling molecule (Fzd1) that controls activation of β -catenin and its

Table 3 Genes upregulated in cDCs

Gene	DC expression	Macrophage expression
<i>Anep</i>	1,682.8 ± 197.7	87.1 ± 20.7
<i>Bri3bp</i>	814.3 ± 86.3	177 ± 44.1
<i>Cbfa2t3</i>	1,266.3 ± 100.8	208.5 ± 52.5
<i>Ciita</i>	1,692 ± 190.1	121.4 ± 46.8
<i>Cnn2</i>	1,884.8 ± 271.2	230.7 ± 54.7
<i>Dpp4</i>	2,567.1 ± 360	72.3 ± 29.6
<i>Fgl2</i>	1,276.4 ± 326	90.2 ± 26.3
<i>H2-Aa</i>	13,267.3 ± 555.7	1,632.6 ± 1173.7
<i>H2-Ab1</i>	10,299.7 ± 490.6	1,093.6 ± 755.3
<i>H2-DMb2</i>	2,491.8 ± 305.6	400.5 ± 67.6
<i>H2-Eb1</i>	7,165.4 ± 608	704.4 ± 458.9
<i>H2-Q6</i>	1,481.4 ± 149.9	288 ± 48.4
<i>Hao</i>	653.2 ± 59.4	152.3 ± 24.9
<i>Jak2</i>	2,300 ± 234.7	331.9 ± 51.5
<i>Napsa</i>	1,616.4 ± 237	190.9 ± 49.7
<i>Pstpip1</i>	475.1 ± 42.7	104.4 ± 16.4
<i>Runx3</i>	672.8 ± 151.1	100.9 ± 11.3
<i>Spint2</i>	773.6 ± 166	139.4 ± 8.4
<i>Tbc1d8</i>	2009.8 ± 209.5	219.3 ± 75.8

Genes of the transcriptome significantly upregulated in cDCs (excluding nonlymphoid tissue CD11b⁺ cDC subsets; FDR ≤ 0.05 (t-test)) relative to their expression in macrophages (populations as in Table 2). Data are representative of at least three experiments (average ± s.e.m.).

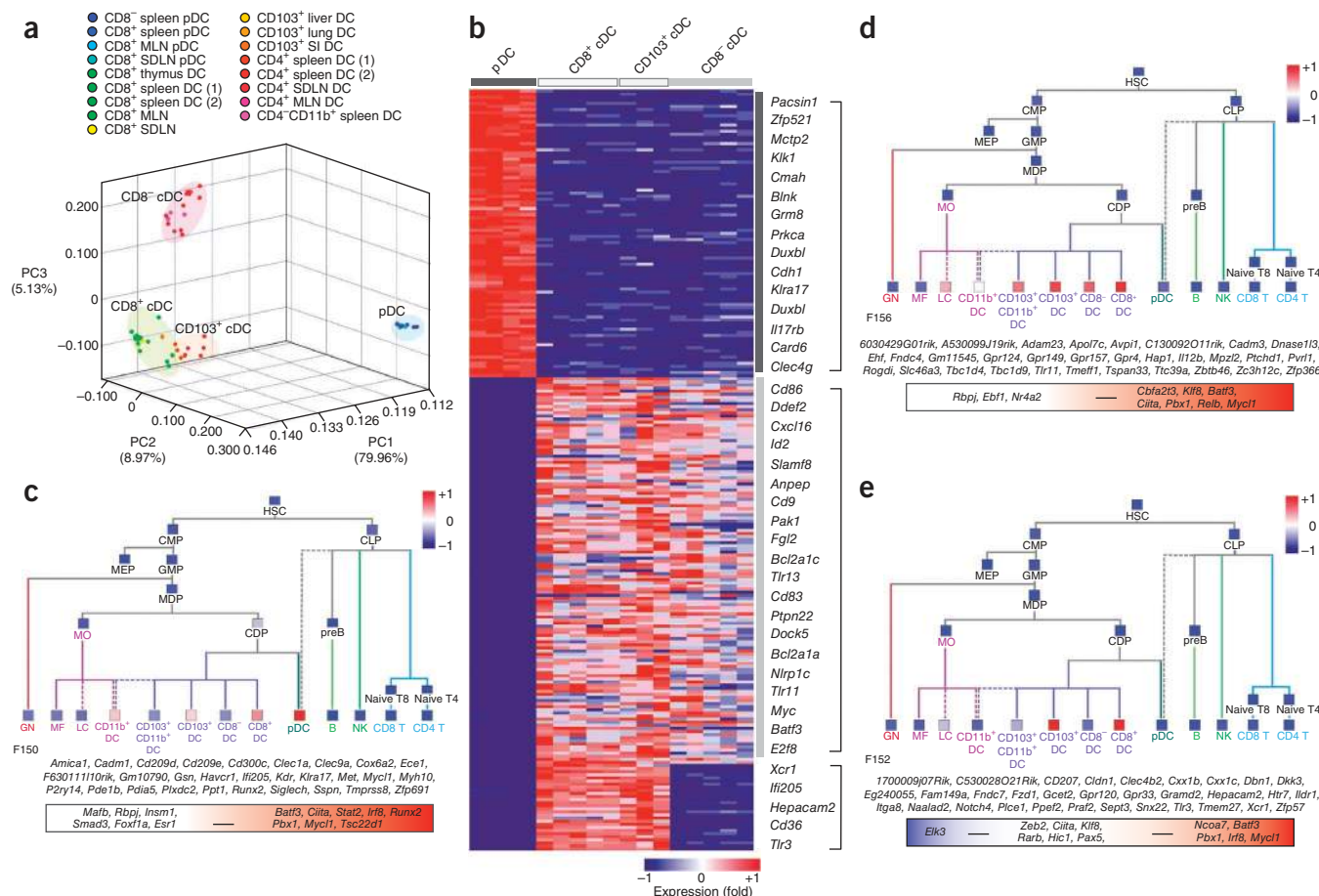


Figure 3 Unique gene signatures characterize distinct tissue DC clusters. **(a)** PCA of the 15% of genes with the most variable expression in pDCs, CD8⁺ cDCs, CD8⁻ cDCs and CD103⁺ cDCs. **(b)** Heat map of genes significantly upregulated by at least twofold relative to their expression in the comparison population (FDR ≤ 0.05 (*t*-test)) and not expressed in the exclusion population (according to the QC95 value), for pDCs versus cDCs, cDCs versus pDCs, and CD8⁺ cDCs and CD103⁺ cDCs versus pDCs or CD8⁻ cDCs (full gene list, **Supplementary Table 1**; presented as in **Fig. 1b**). **(c–e)** ImmGen Project fine modules, consisting of genes with high coexpression with projection of module F150 (**c**), module F156 (**d**) and module F152 (**e**) across data from the ImmGen Project (mean of each module). Below, genes expressed in each module, with genes encoding regulators predicted with the Ontogenet algorithm outlined in box (red, predicted activators; blue, predicted repressors). HSC, hematopoietic stem cell; CMP, common myeloid progenitor; CLP, common lymphoid progenitor; MEP, megakaryocyte-erythrocyte progenitor; MO, monocyte; preB, pre-B cell; T8 or CD8 T, CD8⁺ T cell; T4 or CD4 T, CD4⁺ T cell; GN, granulocyte; B, B cell; NK, natural killer cell. Data are representative of at least three experiments with three or more replicates (unless noted otherwise in **Table 1**).

translocation to the nucleus (**Supplementary Figs. 4 and 6**). *Fzd1* was expressed specifically in CD103⁺CD11b⁻ cDCs from the small intestine and was absent from CD103⁺CD11b⁺ cDCs and CD103⁻CD11b⁺ cDCs from the small intestine (**Supplementary Fig. 6**). Activation of β-catenin and its translocation to the nucleus can control the ability of DCs to promote T cell tolerance in the intestine⁵⁰. Future studies should examine the contribution of Fzd1 to the immunomodulatory function of CD103⁻CD11b⁺ cDCs in the small intestine.

In contrast, the CD103⁻CD11b⁺ cDCs clustered near macrophages and away from other DCs in the PCA plot (**Fig. 4a**). Consistent with the PCA results, we found that CD103⁺CD11b⁻ and CD103⁺CD11b⁺ DCs from the small intestine expressed 100% of the core cDC genes and also expressed the cDC-specific proteins c-Kit, Flt3, BTLA and CD26 on the cell surface (**Fig. 4b–d** and **Supplementary Fig. 6**), which suggested that these two subsets belonged to the lineage. In contrast, CD103⁻CD11b⁺ cDCs clustered near macrophages and away from cDCs in the PCA plot (**Fig. 4a**), and they expressed only 40% of the cDC genes and lacked the cDC proteins c-Kit, Flt3, BTLA and CD26 on the cell surface (**Fig. 4b–d** and **Supplementary Fig. 6**),

which suggested that the CD103⁻CD11b⁺ cDCs from the small intestine belonged to the macrophage lineage. Accordingly, focused analysis of macrophage-associated transcripts indicated that the CD103⁻CD11b⁺ cDC population from the small intestine clustered with macrophages (E.L.G. *et al.*, data not shown). Together these results established that the present phenotypic definition of DCs, based on expression of MHC class II and CD11c, is not sufficient to identify tissue DCs and that the use of the cDC gene signature identified here may provide a new means of distinguishing CD11b⁺ cDCs from macrophages in nonlymphoid tissues.

Unique transcriptional signature of migratory DCs

Tissue-draining lymph nodes contain blood-derived DCs that include pDCs, CD8⁺ cDCs and CD8⁻ cDCs, also called 'lymph node-resident DCs', as well as nonlymphoid-tissue CD103⁺ cDCs and CD11b⁺ cDCs that have migrated from the drained tissue, also called 'tissue-migratory cDCs'⁶. The mechanisms that control the migration and function of nonlymphoid-tissue cDCs in the draining lymph nodes in response to tissue injury or tissue immunization are starting to be

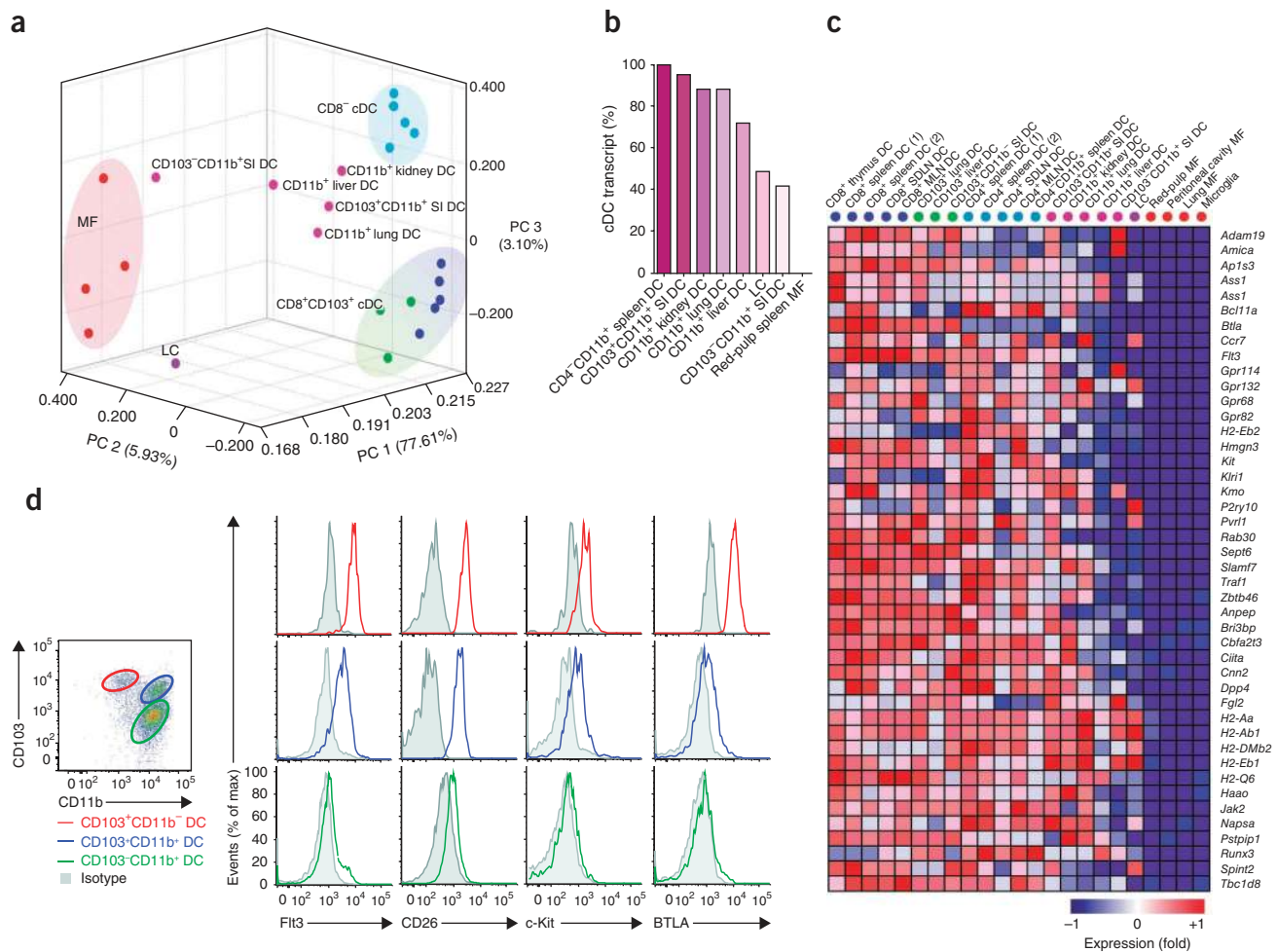


Figure 4 Heterogeneity of nonlymphoid-tissue CD11b⁺ cDCs. **(a)** PCA of the 15% of genes with the most variable expression in lymphoid-tissue CD8⁺ cDCs and CD8⁺ cDCs, nonlymphoid-tissue CD103⁺ cDCs, nonlymphoid-tissue CD11b⁺ cDCs, epidermal LCs and macrophages (population means; colors match those above **c**). **(b)** Frequency of core transcripts and transcripts significantly upregulated in cDCs relative to their expression in macrophages (identified in **Fig. 2**) in CD11b⁺ cDC subsets and red-pulp macrophages, among all transcript present (in each subset). **(c)** Heat map of genes significantly upregulated in cDCs relative to their expression in macrophages. **(d)** Expression of the products of core cDC genes in single-cell suspensions of the small intestine, analyzed by flow cytometry: CD103 and CD11b on CD45⁺CD11c⁺ cDCs from the lamina propria that expressed MHC class II and lacked staining with the DNA-intercalating dye DAPI (far left); and Flt3, CD26, c-Kit and BTLA on CD103⁺CD11b⁺ cells, CD103⁺CD11b⁺ cells and CD103⁺CD11b⁺ cells. Data are representative of three independent experiments with three or more replicates (unless noted otherwise in **Table 1**).

elucidated; however, far less is known about the gene program that controls the ability of cDCs to leave peripheral tissues and migrate to the draining lymph nodes or the gene regulators that control the immunological function of migratory cDCs in the uninflamed state⁶. We analyzed the transcriptional program of tissue cDCs before their migration to the draining lymph nodes (parent DC population) and after migration to the lymph nodes, as well as that of lymph node-resident cDCs. Notably, we found that migratory cDCs segregated together in the PCA plot regardless of their cellular or tissue origin, segregated away from the parent cDC populations that populated the drained tissue (**Fig. 5a**) and shared a similar transcriptional program (**Fig. 5b–e**). Migratory CD11b⁺ cDCs and migratory LCs clustered together with CD103⁺ migratory cDCs in the PCA plot (**Fig. 5a**), which suggested that among tissue CD11b⁺ cDCs, those that migrated in the steady state may have represented the true cDCs. In addition, we found that in contrast to tissue CD11b⁺ cDCs, which had moderate expression of the specific gene *Flt3*, migratory CD11b⁺ cDCs always had high expression of *Flt3*. Specifically, epidermal LCs,

which develop independently of Flt3 and Flt3L¹⁹ and have very low expression of *Flt3* in tissues, showed considerable upregulation of *Flt3* once they reached the lymph nodes (**Supplementary Fig. 7**), which suggested a critical role for Flt3 in the homeostasis or function of steady-state migratory cDCs.

We also found that tissue-migratory cDCs upregulated some genes encoding molecules dedicated to the dampening of immune responses (**Fig. 6**). As such ‘dampening genes’ can also be upregulated in response to injury, we further compared steady-state migratory cDCs with poly(I:C)-activated cDCs (**Fig. 6a**). As expected, poly(I:C)-activated and steady-state tissue-migratory cDCs upregulated *Cd40*, which encodes the costimulatory molecule CD40 that has been reported on steady-state migratory LCs⁵¹ (**Fig. 6a**); however, steady-state migratory cDCs did not upregulate genes encoding inflammatory cytokines (**Fig. 6b**) and had higher expression of genes encoding immunomodulatory molecules than did poly(I:C)-activated cDCs (**Fig. 6a**). The genes encoding immunomodulatory molecules that were upregulated in steady-state migratory cDCs included

those encoding molecules known to suppress T cell function either directly, such as PD-L1 (encoded by *Cd274*)⁵², or through the production or activation of immunosuppressive cytokines, such as the TGF- β -activating integrin β_8 (encoded by *Itgb8*)⁵³. Other upregulated

genes encoded proteins known to diminish the activation and cytokine production of DCs, including SOCS2, a TLR-responsive molecule that regulates the release of cytokines from DCs via STAT3 modulation⁵⁴; the inhibitory protein PIAS3 also known to modulate

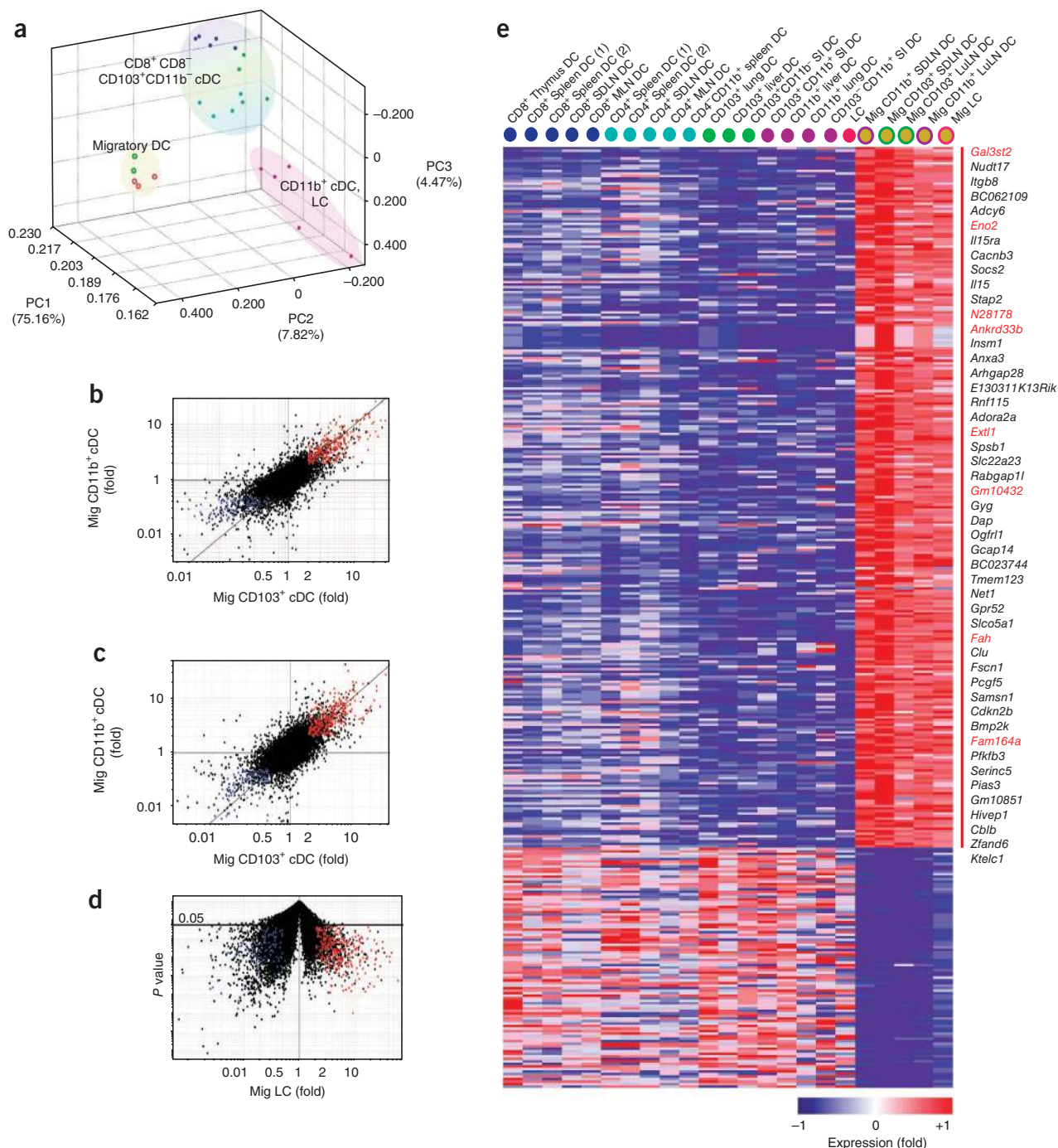


Figure 5 Tissue-migratory cDCs upregulate a unique gene signature regardless of tissue or cellular origin. **(a)** PCA of the 15 genes with the most variable expression by lymphoid tissue-resident CD8⁺ cDCs and CD8⁻ cDCs, nonlymphoid-tissue CD103⁺ cDCs, nonlymphoid-tissue CD11b⁺ cDCs, epidermal LCs, migratory (Mig) LCs isolated from the skin-draining lymph nodes, and migratory CD103⁺ and CD11b⁺ cDCs isolated from skin-draining and lung-draining lymph nodes (population means). **(b)** Genes with significant upregulation of twofold or more (red) or significant downregulation by 50% or more (blue) in migratory CD103⁺ cDCs and CD11b⁺ cDCs, relative to that in nonlymphoid tissue-resident CD103⁺ and CD11b⁺ cDCs. $P \leq 0.05$ (t -test). **(c)** Gene expression in migratory CD103⁺ cDCs and CD11b⁺ cDCs, relative to that in lymphoid tissue-resident CD8⁺ cDCs and CD8⁻ cDCs (colors as in **b**). **(d)** Gene expression in migratory LCs, relative to that in epidermal LCs (colors as in **b**). **(e)** Heat map of the results in **b–d**; right margin, genes (Supplementary Table 2) upregulated at least fivefold in migratory cDCs relative to the mean expression in nonlymphoid-tissue cDCs (red font, transcripts not expressed in nonlymphoid-tissue cDCs, according to the QC95 value). LuLN, lung-draining lymph node. Data are representative of three experiments with three or more replicates (unless noted otherwise in Table 1).

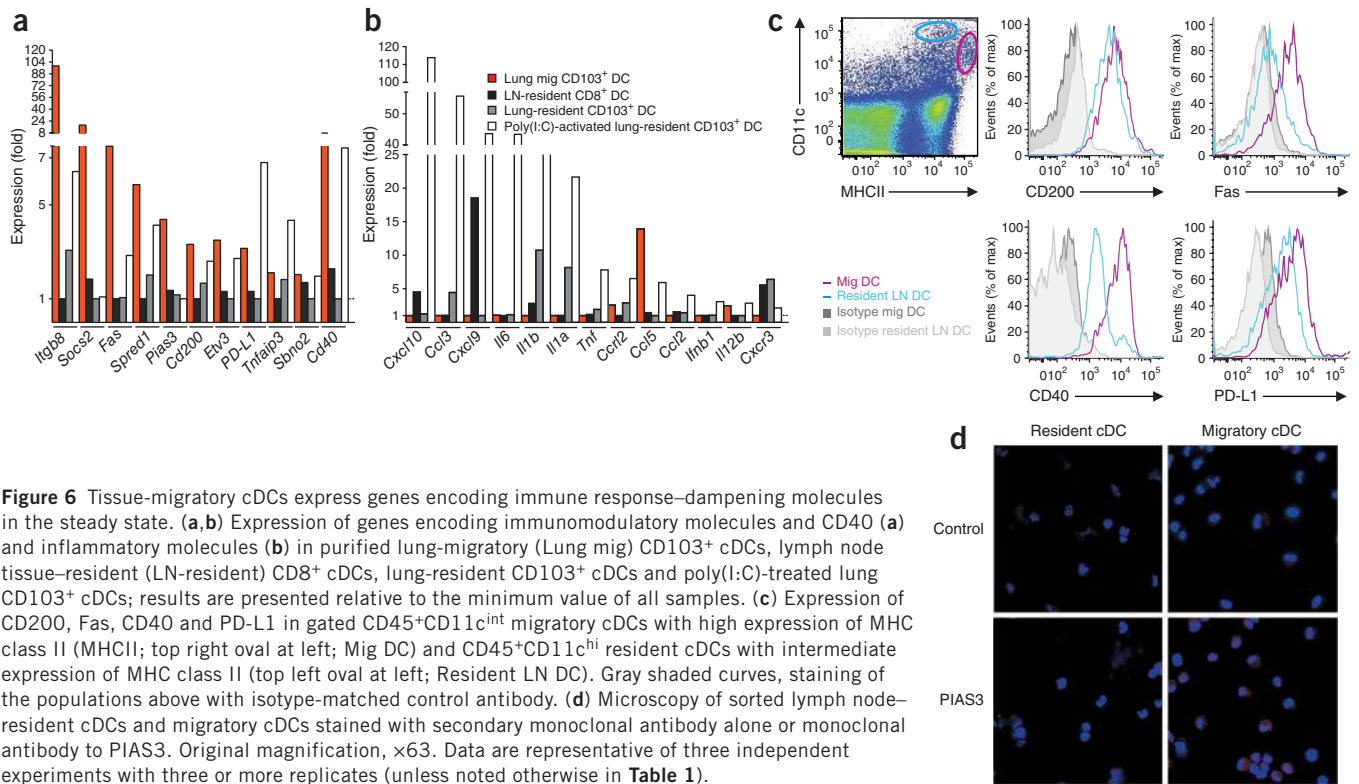


Figure 6 Tissue-migratory cDCs express genes encoding immune response-dampening molecules in the steady state. **(a,b)** Expression of genes encoding immunomodulatory molecules and CD40 **(a)** and inflammatory molecules **(b)** in purified lung-migratory (Lung mig) CD103⁺ cDCs, lymph node tissue-resident (LN-resident) CD8⁺ cDCs, lung-resident CD103⁺ cDCs and poly(I:C)-treated lung CD103⁺ cDCs; results are presented relative to the minimum value of all samples. **(c)** Expression of CD200, Fas, CD40 and PD-L1 in gated CD45⁺CD11c^{int} migratory cDCs with high expression of MHC class II (MHCII; top right oval at left; Mig DC) and CD45⁺CD11c^{hi} resident cDCs with intermediate expression of MHC class II (top left oval at left; Resident LN DC). Gray shaded curves, staining of the populations above with isotype-matched control antibody. **(d)** Microscopy of sorted lymph node-resident cDCs and migratory cDCs stained with secondary monoclonal antibody alone or monoclonal antibody to PIAS3. Original magnification, $\times 63$. Data are representative of three independent experiments with three or more replicates (unless noted otherwise in **Table 1**).

phosphorylation of STAT3 and expression of the transcription factor NF- κ B⁵⁵; and CD200, an immunoregulatory molecule known to diminish the proinflammatory activation of DCs after binding to its receptor, which is also expressed on DCs⁵⁶. Furthermore, steady-state migratory cDCs upregulated genes encoding molecules important in diminishing the survival of DCs, including cell-death receptor Fas (CD95)^{57,58}. By flow cytometry and immunofluorescence analysis, we confirmed expression of Fas, CD200, PD-L1, PIAS3 and CD40 protein in steady-state tissue-migratory cDCs (**Fig. 6c,d**). On the basis of these data, we speculate that cDCs that leave nonlymphoid tissues in the steady state upregulate genes that encode components of a transcriptional immunomodulatory program that may prevent the induction of adaptive immune response to self tissue antigens. The functional relevance of the immunomodulatory signature of migratory DCs must be confirmed experimentally.

DISCUSSION

Here we have provided a comprehensive comparative analysis of the transcriptome of DC precursors and tissue DCs across the entire immune system. The results of our study have helped to identify the transcriptional network that accompanies the lineage commitment and diversification of DCs, as well as a DC-specific signature that distinguishes cDCs from macrophages in tissues. They have also elucidated the relationship between lymphoid-tissue and nonlymphoid-tissue DC subsets and predicted regulators of DC diversity, as well as a transcriptional immunomodulatory program expressed specifically during the migration of steady-state tissue DCs to the draining lymph nodes.

To gain knowledge of the transcriptional network that controls the commitment of myeloid cells to the DC lineage, we analyzed the transcriptional network associated with three key DC-differentiation checkpoints: common myeloid progenitor to MDP; MDP to CDP; and CDP to either pDC or CD8⁺ or CD8⁻ cDC. This analysis identified genes encoding a group of transcriptional activators, including *Runx2*,

Bcl11a and *Klf8*, whose expression increased specifically during the commitment of MDPs to CDPs but not during their commitment to monocytes, which suggested their potential key role in driving the commitment of myeloid cells to DC-restricted precursors and away from monocytes *in vivo*. Notably, most of these genes encoded molecules shown to control the pDC lineage, which suggested that differentiation into pDCs represents the 'default' pathway for CDPs. We also characterized the transcriptional networks that accompanied the differentiation of CDPs into pDC, CD8⁺ cDC and CD8⁻ cDC subsets and identified several gene candidates whose products may drive DC lineage diversification *in vivo*.

One of the main controversies in the DC literature is the distinct contribution of cDCs versus macrophages to tissue immunity. This confusion is partly a consequence of the paucity of markers available to distinguish between these two cell types, which has led researchers to use 'promiscuous' markers such as MHC class II, CD11c and F4/80 to assess cDC- or macrophage-specific function⁹. We have identified a core cDC gene signature shared by lymphoid-tissue CD8⁻ cDCs and CD8⁺ cDCs and nonlymphoid-tissue CD103⁺ cDCs and absent from tissue macrophages. The cDC-specific genes included *Zbtb46*, *Flt3*, *Kit* and *Ccr7*. The identification of *Kit* as part of the cDC-specific signature was unexpected, as c-Kit and its ligand have never been shown to have an intrinsic role in cDC development *in vivo*. Additional studies are needed to identify the role, if any, of c-Kit in the differentiation, function and homeostasis of DCs *in vivo*. Notably, the use of the cDC gene signature helped delineate the heterogeneity of nonlymphoid-tissue CD11b⁺ cDCs and identified a contaminating macrophage population that would not have been detected with the phenotypical markers now used to define DC populations *in vivo*.

We also established that among cDCs, lymphoid-tissue CD8⁺ cDCs and nonlymphoid-tissue CD103⁺ cDCs shared a gene signature regardless of the tissue environment in which they resided. The gene signature of CD8⁺ cDCs and CD103⁺ cDCs was absent from the rest of the DCs, including

pDCs, CD8⁺ cDCs and CD103⁺ cDCs in the same tissues. These results established CD8⁺ cDCs and CD103⁺ cDCs as a distinct lineage subset and identified the gene regulators that may drive their differentiation, homeostasis and function. With the algorithm Ontogenet, developed for the data set of the ImmGen Project (V.J. *et al.*, data not shown), we identified modules of genes with substantial coexpression that had specific and different expression in each DC subset. Specifically, we found that modules F150, F156 and F152 were upregulated in pDCs, cDCs and CD8⁺ cDCs and CD103⁺ cDCs, respectively, and identified candidate regulatory programs that could be used to predict their expression pattern and therefore may drive the functional specialization of DCs *in vivo*.

Notably, we found that regardless of tissue or cellular origin, non-lymphoid-tissue CD103⁺ cDCs and CD11b⁺ cDCs as well as epidermal LCs that migrated to the draining lymph nodes in the steady state upregulated a shared gene signature. Some of the genes with the greatest upregulation have been linked to the production of immunosuppressive cytokines by DCs, dampening of DC activation and diminished DC survival known to lead to the dampening of T cell activation. These results were consistent with the potential role of steady-state migratory cDCs in the induction or maintenance of the regulatory T cell response³ and identified candidate molecules that may participate in the control of tolerance to self antigens *in vivo*.

The results of our study have provided a comprehensive characterization of the transcriptional network of the DC lineage. Our findings should aid in the development of new genetic tools, such as inducible gene regulation *in vivo* and lineage tracing of genetically marked, defined myeloid precursor populations, to further elucidate the developmental complexity of the phagocyte system. Moreover, the availability of data sets from the ImmGen Project will now permit further investigation into DC gene-expression networks and help delineate the transcriptional program that controls DC function in the steady state and injured state.

METHODS

Methods and any associated references are available in the online version of the paper.

Accession codes. GEO: microarray data, GSE15907.

Note: Supplementary information is available in the online version of the paper.

ACKNOWLEDGMENTS

We thank colleagues of the ImmGen Project, especially the technical team, including M. Painter, J. Ericson and S. Davis, for contributions; C. Benoist for contributions to the design and writing of the manuscript; and eBioscience and Affymetrix for support of the ImmGen Project. Supported by the National Institute of Allergy and Infectious Diseases of the US National Institutes of Health (R24 AI072073 to the ImmGen Project (led by C. Benoist); AI080884 and HL086899 to M.M.; JDRF172010770 and DP2DK083052-01 to B.D.B.; DK074500 and AI045757 to S.J.T.; HL69438, DK056638, HL097819 and HL097700 to P.S.F.; and U54CA149145 to V.J.).

AUTHOR CONTRIBUTIONS

J.C.M. did experiments and wrote the paper; M.M. designed experiments and wrote the paper; B.D.B. provided intellectual input, did computational analyses and helped write the paper; T.S. did computation analyses and identified all modules; E.L.G. purified macrophage populations and provided intellectual input; V.J. did computation analyses and, together with T.S., designed Ontogenet; A.C. and G.P. did computation analyses; M.L. did experiments; K.G.E., J.H., D.H., A.C. and J.P. purified DC populations; M.G. purified macrophage populations; M.B. and A.B.-P. purified DC and macrophage populations; P.S.F. provided intellectual input; and G.J.R. and S.J.T. provided intellectual input for experimental design.

COMPETING FINANCIAL INTERESTS

The authors declare no competing financial interests.

Published online at <http://www.nature.com/dofinder/10.1038/ni.2370>.

Reprints and permissions information is available online at <http://www.nature.com/reprints/index.html>.

1. Banchereau, J. & Steinman, R.M. Dendritic cells and the control of immunity. *Nature* **392**, 245–252 (1998).
2. Steinman, R.M. & Banchereau, J. Taking dendritic cells into medicine. *Nature* **449**, 419–426 (2007).
3. Steinman, R.M., Hawiger, D. & Nussenzweig, M.C. Tolerogenic dendritic cells. *Annu. Rev. Immunol.* **21**, 685–711 (2003).
4. Guermontprez, P., Valladeau, J., Zitvogel, L., Thery, C. & Amigorena, S. Antigen presentation and T cell stimulation by dendritic cells. *Annu. Rev. Immunol.* **20**, 621–667 (2002).
5. Trombetta, E.S. & Mellman, I. Cell biology of antigen processing *in vitro* and *in vivo*. *Annu. Rev. Immunol.* **23**, 975–1028 (2005).
6. Randolph, G.J., Angeli, V. & Swartz, M.A. Dendritic-cell trafficking to lymph nodes through lymphatic vessels. *Nat. Rev. Immunol.* **5**, 617–628 (2005).
7. Cyster, J.G. Chemokines and the homing of dendritic cells to the T cell areas of lymphoid organs. *J. Exp. Med.* **189**, 447–450 (1999).
8. Hashimoto, D., Miller, J. & Merad, M. Dendritic cell and macrophage heterogeneity *in vivo*. *Immunity* **35**, 323–335 (2011).
9. Geissmann, F., Gordon, S., Hume, D.A., Mowat, A.M. & Randolph, G.J. Unravelling mononuclear phagocyte heterogeneity. *Nat. Rev. Immunol.* **10**, 453–460 (2010).
10. Heath, W.R. & Carbone, F.R. Dendritic cell subsets in primary and secondary T cell responses at body surfaces. *Nat. Immunol.* **10**, 1237–1244 (2009).
11. Shortman, K. & Heath, W.R. The CD8⁺ dendritic cell subset. *Immunol. Rev.* **234**, 18–31 (2010).
12. Reizis, B., Bunin, A., Ghosh, H.S., Lewis, K.L. & Sisirak, V. Plasmacytoid dendritic cells: recent progress and open questions. *Annu. Rev. Immunol.* **29**, 163–183 (2011).
13. Helft, J., Ginhoux, F., Bogunovic, M. & Merad, M. Origin and functional heterogeneity of non-lymphoid tissue dendritic cells in mice. *Immunol. Rev.* **234**, 55–75 (2010).
14. Coombes, J.L. & Powrie, F. Dendritic cells in intestinal immune regulation. *Nat. Rev. Immunol.* **8**, 435–446 (2008).
15. Fogg, D.K. *et al.* A clonogenic bone marrow progenitor specific for macrophages and dendritic cells. *Science* **311**, 83–87 (2006).
16. Liu, K. *et al.* *In vivo* analysis of dendritic cell development and homeostasis. *Science* **324**, 392–397 (2009).
17. Onai, N. *et al.* Identification of clonogenic common Flt3⁺M-CSFR⁺ plasmacytoid and conventional dendritic cell progenitors in mouse bone marrow. *Nat. Immunol.* **8**, 1207–1216 (2007).
18. Naik, S.H. *et al.* Development of plasmacytoid and conventional dendritic cell subtypes from single precursor cells derived *in vitro* and *in vivo*. *Nat. Immunol.* **8**, 1217–1226 (2007).
19. Ginhoux, F. *et al.* The origin and development of nonlymphoid tissue CD103⁺ DCs. *J. Exp. Med.* **206**, 3115–3130 (2009).
20. Lewis, K.L. *et al.* Notch2 receptor signaling controls functional differentiation of dendritic cells in the spleen and intestine. *Immunity* **35**, 780–791 (2011).
21. Malhotra, D. *et al.* Transcriptional profiling of stroma from inflamed and resting lymph nodes defines immunological hallmarks. *Nat. Immunol.* **13**, 499–510 (2012).
22. Waskow, C. *et al.* The receptor tyrosine kinase Flt3 is required for dendritic cell development in peripheral lymphoid tissues. *Nat. Immunol.* **9**, 676–683 (2008).
23. Aliberti, J. *et al.* Essential role for ICSBP in the *in vivo* development of murine CD8 α ⁺ dendritic cells. *Blood* **101**, 305–310 (2003).
24. DiMartino, J.F. *et al.* The Hox cofactor and proto-oncogene Pbx1 is required for maintenance of definitive hematopoiesis in the fetal liver. *Blood* **98**, 618–626 (2001).
25. Wu, L., Nichogiannopoulou, A., Shortman, K. & Georgopoulos, K. Cell-autonomous defects in dendritic cell populations of Ikaros mutant mice point to a developmental relationship with the lymphoid lineage. *Immunity* **7**, 483–492 (1997).
26. McKenna, H.J. *et al.* Mice lacking flt3 ligand have deficient hematopoiesis affecting hematopoietic progenitor cells, dendritic cells, and natural killer cells. *Blood* **95**, 3489–3497 (2000).
27. Carotta, S. *et al.* The transcription factor PU.1 controls dendritic cell development and Flt3 cytokine receptor expression in a dose-dependent manner. *Immunity* **32**, 628–641 (2010).
28. Laouar, Y., Welte, T., Fu, X.Y. & Flavell, R.A. STAT3 is required for Flt3L-dependent dendritic cell differentiation. *Immunity* **19**, 903–912 (2003).
29. Reizis, B. Regulation of plasmacytoid dendritic cell development. *Curr. Opin. Immunol.* **22**, 206–211 (2010).
30. Ohtsuka, H. *et al.* Bcl6 is required for the development of mouse CD4⁺ and CD8 α ⁺ dendritic cells. *J. Immunol.* **186**, 255–263 (2011).
31. Meredith, M.M. *et al.* Expression of the zinc finger transcription factor zDC (Zbtb46, Btbd4) defines the classical dendritic cell lineage. *J. Exp. Med.* **209**, 1153–1165 (2012).
32. Satpathy, A.T. *et al.* Zbtb46 expression distinguishes classical dendritic cells and their committed progenitors from other immune lineages. *J. Exp. Med.* **209**, 1135–1152 (2012).
33. Ohl, L. *et al.* CCR7 governs skin dendritic cell migration under inflammatory and steady-state conditions. *Immunity* **21**, 279–288 (2004).
34. Lyman, S.D. *et al.* Identification of soluble and membrane-bound isoforms of the murine flt3 ligand generated by alternative splicing of mRNAs. *Oncogene* **10**, 149–157 (1995).
35. Broxmeyer, H.E. *et al.* The kit receptor and its ligand, steel factor, as regulators of hemopoiesis. *Cancer Cells* **3**, 480–487 (1991).
36. del Rio, M.L., Lucas, C.L., Buhler, L., Rayat, G. & Rodriguez-Barbosa, J.I. HVEM/LIGHT/BTLA/CD160 cosignaling pathways as targets for immune regulation. *J. Leukoc. Biol.* **87**, 223–235 (2010).
37. Hochrein, H. *et al.* Differential production of IL-12, IFN- α , and IFN- γ by mouse dendritic cell subsets. *J. Immunol.* **166**, 5448–5455 (2001).

38. Sung, S.S. *et al.* A major lung CD103 (α_E)- β_7 integrin-positive epithelial dendritic cell population expressing Langerin and tight junction proteins. *J. Immunol.* **176**, 2161–2172 (2006).
39. Longhi, M.P. *et al.* Dendritic cells require a systemic type I interferon response to mature and induce CD4⁺ Th1 immunity with poly IC as adjuvant. *J. Exp. Med.* **206**, 1589–1602 (2009).
40. Jelinek, I. *et al.* TLR3-specific double-stranded RNA oligonucleotide adjuvants induce dendritic cell cross-presentation, CTL responses, and antiviral protection. *J. Immunol.* **186**, 2422–2429 (2011).
41. Lauterbach, H. *et al.* Mouse CD8 α^+ DCs and human BDCA3⁺ DCs are major producers of IFN- λ in response to poly IC. *J. Exp. Med.* **207**, 2703–2717 (2010).
42. Dörner, B.G. *et al.* Selective expression of the chemokine receptor XCR1 on cross-presenting dendritic cells determines cooperation with CD8⁺ T cells. *Immunity* **31**, 823–833 (2009).
43. Bachem, A. *et al.* Superior antigen cross-presentation and XCR1 expression define human CD11c⁺CD141⁺ cells as homologues of mouse CD8⁺ dendritic cells. *J. Exp. Med.* **207**, 1273–1281 (2010).
44. Schmucker, D. *et al.* *Drosophila* Dscam is an axon guidance receptor exhibiting extraordinary molecular diversity. *Cell* **101**, 671–684 (2000).
45. Watson, F.L. *et al.* Extensive diversity of Ig-superfamily proteins in the immune system of insects. *Science* **309**, 1874–1878 (2005).
46. Varol, C. *et al.* Intestinal lamina propria dendritic cell subsets have different origin and functions. *Immunity* **31**, 502–512 (2009).
47. Bogunovic, M. *et al.* Origin of the lamina propria dendritic cell network. *Immunity* **31**, 513–525 (2009).
48. Schulz, O. *et al.* Intestinal CD103⁺, but not CX3CR1⁺, antigen sampling cells migrate in lymph and serve classical dendritic cell functions. *J. Exp. Med.* **206**, 3101–3114 (2009).
49. Varol, C., Zigmund, E. & Jung, S. Securing the immune tightrope: mononuclear phagocytes in the intestinal lamina propria. *Nat. Rev. Immunol.* **10**, 415–426 (2010).
50. Manicassamy, S. *et al.* Activation of β -catenin in dendritic cells regulates immunity versus tolerance in the intestine. *Science* **329**, 849–853 (2010).
51. Henri, S. *et al.* The dendritic cell populations of mouse lymph nodes. *J. Immunol.* **167**, 741–748 (2001).
52. Sharpe, A.H., Wherry, E.J., Ahmed, R. & Freeman, G.J. The function of programmed cell death 1 and its ligands in regulating autoimmunity and infection. *Nat. Immunol.* **8**, 239–245 (2007).
53. Travis, M.A. *et al.* Loss of integrin $\alpha_E\beta_8$ on dendritic cells causes autoimmunity and colitis in mice. *Nature* **449**, 361–365 (2007).
54. Posselt, G., Schwarz, H., Duschl, A. & Horejs-Hoeck, J. Suppressor of cytokine signaling 2 is a feedback inhibitor of TLR-induced activation in human monocyte-derived dendritic cells. *J. Immunol.* **187**, 2875–2884 (2011).
55. Yagil, Z. *et al.* The enigma of the role of protein inhibitor of activated STAT3 (PIAS3) in the immune response. *Trends Immunol.* **31**, 199–204 (2010).
56. Minas, K. & Liversidge, J. Is the CD200/CD200 receptor interaction more than just a myeloid cell inhibitory signal? *Crit. Rev. Immunol.* **26**, 213–230 (2006).
57. Chen, M. *et al.* Dendritic cell apoptosis in the maintenance of immune tolerance. *Science* **311**, 1160–1164 (2006).
58. Stranges, P.B. *et al.* Elimination of antigen-presenting cells and autoreactive T cells by Fas contributes to prevention of autoimmunity. *Immunity* **26**, 629–641 (2007).

ImmGen Consortium:

Emmanuel L Gautier^{12,13}, Claudia Jakubczik¹², Gwendalyn J Randolph^{12,13}, Adam J Best¹⁴, Jamie Knell¹⁴, Ananda Goldrath¹⁴, Jennifer Miller¹², Brian Brown¹², Miriam Merad¹², Vladimir Jojic¹⁵, Daphne Koller¹⁵, Nadia Cohen¹⁶, Patrick Brennan¹⁶, Michael Brenner¹⁶, Tal Shay¹⁷, Aviv Regev¹⁷, Anne Fletcher¹⁸, Kutlu Elpek¹⁸, Angelique Bellemare-Pelletier¹⁸, Deepali Malhotra¹⁸, Shannon Turley¹⁸, Radu Jianu¹⁹, David Laidlaw¹⁹, Jim Collins²⁰, Kavitha Narayan²¹, Katelyn Sylvia²¹, Joonsoo Kang²¹, Roi Gazit²², Derrick J Rossi²², Francis Kim²³, Tata Nageswara Rao²³, Amy Wagers²³, Susan A Shinton²⁴, Richard R Hardy²⁴, Paul Monach²⁵, Natalie A Bezman²⁶, Joseph C Sun²⁶, Charlie C Kim²⁶, Lewis L Lanier²⁶, Tracy Heng²⁷, Taras Kreslavsky¹⁵, Michio Painter²⁷, Jeffrey Ericson²⁷, Scott Davis²⁷, Diane Mathis²⁷ & Christophe Benoist²⁷

¹²Mount Sinai Hospital, New York, New York, USA. ¹³Department of Pathology & Immunology, Washington University, St. Louis, Missouri, USA. ¹⁴Division of Biological Sciences, University of California San Diego, La Jolla, California, USA. ¹⁵Computer Science Department, Stanford University, Stanford, California, USA. ¹⁶Division of Rheumatology, Immunology and Allergy, Brigham and Women's Hospital, Boston, Massachusetts, USA. ¹⁷Broad Institute, Cambridge, Massachusetts, USA. ¹⁸Dana-Farber Cancer Institute and Harvard Medical School, Boston, Massachusetts, USA. ¹⁹Computer Science Department, Brown University, Providence, Rhode Island, USA. ²⁰Department of Biomedical Engineering, Howard Hughes Medical Institute, Boston University, Boston, Massachusetts, USA. ²¹University of Massachusetts Medical School, Worcester, Massachusetts, USA. ²²Department of Stem Cell and Regenerative Biology, Harvard University, and Program in Cellular and Molecular Medicine, Children's Hospital, Boston, Massachusetts, USA. ²³Joslin Diabetes Center, Boston, Massachusetts, USA. ²⁴Fox Chase Cancer Center, Philadelphia, Pennsylvania, USA. ²⁵Department of Medicine, Boston University, Boston, Massachusetts, USA. ²⁶Department of Microbiology & Immunology, University of California San Francisco, San Francisco, California, USA. ²⁷Department of Microbiology & Immunobiology, Division of Immunology, Harvard Medical School, Boston, Massachusetts, USA.

ONLINE METHODS

Mice. All cells were obtained from 6-week-old male C57BL/6J mice from The Jackson Laboratory, except LCs and migratory LCs, which were isolated from C57BL/6J mice with transgenic expression of langerin linked to enhanced green fluorescent protein to aid in the purification of langerin-positive LCs⁵⁹. All mice were housed in specific pathogen-free facilities at the Mount Sinai School of Medicine facility. Experiments involving mice were approved by the Animal Care and Use Committee of the Mount Sinai School of Medicine.

Cell sorting and flow cytometry. All cells were purified by the standardized sorting protocol of the ImmGen Project ([http://www.immgen.org/Protocols/ImmGen Cell prep and sorting SOP.pdf](http://www.immgen.org/Protocols/ImmGen%20Cell%20prep%20SOP.pdf)) with the appropriate antibodies (identified below). Cells were sorted at the Mount Sinai Flow Cytometry Shared Resource Facility with a FACSaria II (BD) or Influx (BD). The marker combinations used for the sorting of specific populations are available on the ImmGen Project website (**Table 1**). An LSR II (BD) was used for multiparameter analysis of stained cell suspensions, followed by analysis with FlowJo software (Tree Star). Monoclonal antibody (mAb) to mouse CD8 (53-6.7), mAb to CD4 (L3T4), mAb to CD45 (30-F11), mAb to CD11c (N418), mAb to CD11b (M1/70), mAb to I-AI-E (M5/114.15.2), mAb to CD103 (2E7), mAb to CD117 (c-Kit; 2B8), mAb to CD135 (Flt3; A2F10), mAb to BTLA (CD272; 6F7), mAb to CD40 (HM40-3), mAb to CD200 (OX90), mAb to PD-L1 (CD274; MIH5), mAb to rat IgG2a,κ, mAb to IgG2b,κ, mAb to rat IgG2a,κ, mAb to mouse IgG,κ, mAb to rat IgG2a,λ, and mAb to Armenian Hamster IgM,κ were all from eBioscience; mAb to CD95 (Fas; Jo2), mAb to CD26 (H1940112), mAb to Rat IgG2a,κ and Armenian hamster IgG2,λ were all from BD.

Cytospin and immunofluorescence of sorted cells. Viable sorted cells isolated according to expression of MHC class II and CD11c were sorted, spun onto glass slides (with Cytospin) and dried overnight. Slides were fixed for 1 h with 4% paraformaldehyde in PBS, nonspecific binding was blocked by incubation for 1 h with 10% goat serum in 0.1% Triton and 0.1% BSA in PBS, then samples were stained for 48 h at 4 °C, followed by 1 h of incubation at room temperature with goat mAb to mouse PIAS3 (P0117; Sigma) at a dilution of 1:2,000. Alexa Fluor 594-conjugated secondary goat antibody to mouse (A-11005; Invitrogen) was added to slides for 1 h at room temperature. Slides were mounted with DAPI (4,6-diamidino-2-phenylindole) in Fluoro-gel with Tris buffer (Electron Microscopy Sciences). Images were acquired at a magnification of ×63 with a Zeiss Axioplan 2IE microscope and a Zeiss AxioCam MRC color camera and were analyzed with Zeiss AxioVision software.

Microarray analysis, normalization and data analysis. RNA was prepared from cell populations sorted from C57BL/6J mice with Trizol reagent as described⁶⁰. RNA was amplified and hybridized on the Affymetrix Mouse Gene 1.0 ST array according to the manufacturer's procedures. Raw data for all populations were preprocessed and normalized by the robust multi-array average algorithm⁶¹ implemented in the 'Expression File Creator' module in the GenePattern suite⁶². RNA processing and microarray analysis with the Affymetrix MoGene 1.0 ST array was prepared according to standard operating procedures of the ImmGen Project ([http://www.immgen.org/Protocols/Total RNA Extraction with Trizol.pdf](http://www.immgen.org/Protocols/Total%20RNA%20Extraction%20with%20Trizol.pdf); [http://www.immgen.org/Protocols/ImmGen QC Documentation_ALL-DataGeneration_0612.pdf](http://www.immgen.org/Protocols/ImmGen%20QC%20Documentation_ALL-DataGeneration_0612.pdf)).

Identification of transcription factors associated with DC lineage commitment and diversification. The data set was filtered for genes encoding regulators⁶³ with a coefficient of variation of less than 0.5 in population replicates. The regulators expressed by MDPs selected were those genes with expression 1.5-fold greater than their expression in GMPs and CDPs. Genes encoding regulators expressed by CDPs were filtered for those whose expression was upregulated 1.5-fold or more by MDPs and/or GMPs. The 'MDP and/or GMP' classification allows the inclusion of genes whose expression may be increasing in the MDP population as well and thus may still be informative. Conversely, genes encoding regulators were filtered for those whose expression was upregulated 1.5-fold or more in MDPs relative to their expression in CDPs. Those results were further filtered for genes with expression at least 1.5-fold greater than that of the nearest-neighbor monocyte for the identification of upregulated genes encoding molecules important to the DC lineage alone.

Conversely, genes whose expression was upregulated 1.5-fold or more in monocytes relative to that in CDPs were selected for the identification of genes whose expression decreased along the DC lineage. Gene lists were input into the GenePattern module ExpressCluster (<http://cbdm.hms.harvard.edu/LabMembersPages/SD.html>) for the identification of patterns of expression across the GMP, MDP, CDP and monocyte populations.

The data set was filtered for genes encoding regulators with a coefficient of variation of less than 0.5 in these populations⁶³. Results obtained for differentiated DC subsets were compared with those of their nearest developmental neighbor by a two-way analysis of variance Student's *t*-test of normalized expression data corrected with a Benjamini and Hochberg FDR of <0.05 and were further analyzed for the selection of upregulated by at least 1.5-fold in each organ. Thus, pDCs were compared with CD8⁺ cDCs and CD8⁻ cDCs, and CD8⁺ cDCs were compared with CD8⁻ cDCs in the spleen, skin-draining lymph nodes and mesenteric lymph node DCs and results were filtered for genes upregulated at least 1.5-fold in each comparison. The results for pDCs and cDCs were then compared with those of their precursor CDP to identify genes whose expression was upregulated 1.5-fold or more in the precursor cell relative to their expression in pDC and cDC populations.

Generation of the cell-specific gene signatures. Differences in expression were assessed by an unpaired two-way analysis of variance Student's *t*-test on normalized expression data. The *t*-test was controlled for multiple hypothesis with a Benjamini and Hochberg FDR of <0.05. The data set was then filtered for those probes for which the change in expression of any single population mean value of the inclusion group over any single population mean value of the exclusion group was twofold or greater to create signatures of upregulated transcripts. The data set was further filtered for genes for which the exclusion populations had an expression value less than the QC value of 95 (the value at which each population would have a predicted 95% certainty of expressing the gene). These gene signatures were also analyzed for variance across all steady-state leukocyte populations with the analysis of variance (ANOVA) command in the software of the R project for statistical computing. Data were log-transformed before analysis. Data for each population were analyzed by a *post-hoc* pairwise Student's *t*-test, corrected for multiple hypotheses testing with the Bonferroni adjustment. Data from these analyses are provided in **Supplementary Table 1**.

Generation of the gene signature of migratory DCs. The data set was filtered for genes with expression with a coefficient of variation of less than 0.5 in population replicates. For the creation of the gene signature of migratory cDCs, the transcriptome of migratory LCs, lung CD103⁺ cDCs and lung CD11b⁺ cDCs were directly compared with those of their tissue-resident equivalents, and genes with a change in expression of twofold or more that satisfied the Student's *t*-test criterion of a *P* value of less than 0.05 were selected. For the removal of any potential signature that could be created by the lymph node environment, results for the remaining genes were compared for migratory versus resident skin-draining lymph node populations, again with the selection of genes with an increase in expression of twofold or more that satisfied the *t*-test criterion of a *P* value of less than 0.05. This same method was applied to genes with expression upregulated twofold or more in migratory DCs relative to that in resident DCs that satisfied the *t*-test criterion of a *P* value of less than 0.05 for the identification of downregulated signatures. The GenePattern module Multiplot⁶² was used for these analyses.

Generation of gene modules and prediction of module regulators. Expression data were normalized as part of the ImmGen Project pipeline (March 2011 release). Data were log₂-transformed. For genes represented on the array with more than one probe set, only the probe set with the highest mean expression was retained. Of those, only the 7,996 probe sets with a standard deviation higher than 0.5 across the entire data set were used for the clustering.

Super Paramagnetic Clustering⁶⁴ with default parameters was used for clustering, which resulted in 80 stable clusters. The remaining unclustered genes were grouped into a separate cluster (C81). Those are called 'coarse modules C1–C81' here. Each coarse cluster was further clustered by hierarchical clustering into finer clusters, which resulted in 334 fine modules, called 'fine modules F1–F334' here. The expression of each gene was standardized by subtraction of the mean and division by its standard deviation across all



data sets. Results of replicates were averaged. The mean expression of each module was projected on the tree.

The Ontogenet algorithm was developed for the data set of the ImmGen Project (V.J. *et al.*, data not shown). This algorithm finds a regulatory program for each coarse and fine module on the basis of regulator expression and the structure of the lineage tree. A one-sided two-sample Kolmogorov-Smirnov test was applied to the mean expression of each fine module of the ImmGen Project for the identification of modules with significantly induced expression in specific cell groups. The cell groups were pDCs, cDCs, CD8⁻ DCs, CD8⁺ cDCs and CD103⁺ cDCs. The background for each was the result obtained for rest of the samples from the ImmGen Project. A Benjamini Hochberg FDR of ≤ 0.05 was applied to the table of *P* values of all four groups across all fine modules. A hypergeometric test for two groups was used for estimation of the enrichment of fine modules of the ImmGen Project for the four gene signatures. A Benjamini Hochberg FDR of ≤ 0.05 was applied to the table of *P* values of all four groups across all fine modules.

Data analysis and visualization tools. Signature transcripts were clustered and visualized with the HeatMap Viewer or the Hierarchical Clustering tool of the GenePattern genomic analysis platform⁶². For hierarchical clustering, data were log scaled, centered around the mean and clustered with Pearson correlation as a measure and pairwise complete-linkage clustering as a linkage type. Data were centered on rows before visualization. The Immgen PopulationDistances

PCA program (<http://cbdm.hms.harvard.edu/LabMembersPages/SD.html>) was used for PCA. Where indicated, the PCA program was used to identify the 15% of the genes with the greatest difference in expression among subsets by filtering on the basis of a variation of analysis with the geometric standard deviation of populations to 'weight' genes that varied in multiple populations. Data were log-transformed, normalized for gene and subset and filtered for genes with a coefficient of variation of less than 0.5 in each set of sample replicates before visualization. Comparisons of change in expression versus change in expression or of change in expression versus *P* value (*t*-test) were visualized with the Multiplot module of GenePattern⁶². Plots of results from individual genes were created with Prism Software.

59. Kissenpfennig, A. *et al.* Dynamics and function of Langerhans cells *in vivo*: dermal dendritic cells colonize lymph node areas distinct from slower migrating Langerhans cells. *Immunity* **22**, 643–654 (2005).
60. Yamagata, T., Mathis, D. & Benoist, C. Self-reactivity in thymic double-positive cells commits cells to a CD8 α lineage with characteristics of innate immune cells. *Nat. Immunol.* **5**, 597–605 (2004).
61. Irizarry, R.A. *et al.* Summaries of affymetrix GeneChip probe level data. *Nucleic Acids Res.* **31**, e15 (2003).
62. Reich, M. *et al.* GenePattern 2.0. *Nat. Genet.* **38**, 500–501 (2006).
63. Novershtern, N. *et al.* Densely interconnected transcriptional circuits control cell states in human hematopoiesis. *Cell* **144**, 296–309 (2011).
64. Blatt, M., Wiseman, S. & Domany, E. Superparamagnetic clustering of data. *Phys. Rev. Lett.* **76**, 3251–3254 (1996).